MIDDLE EAST TECHNICAL UNIVERSITY

ELECTRICAL AND ELECTRONICS ENGINEERING DEPARTMENT

EE300 SUMMER PRACTICE REPORT

Student Name: Mutlu Ahmetoğlu

Student ID #: 2303865

Summer Practice Institution Name: Middle East Technical University

University Department: Electrical and Electronics Engineering

Research Group: Communication Networks Research Group

Related Field: Telecommunication

Summer Practice Supervisor: Prof. Elif Uysal

Supervisor E-mail: uelif@metu.edu.tr

Summer Practice Date: 06.07.2020-19.08.2020

TABLE OF CONTENTS

1. INTRODUCTION

I have performed my 30-day mandatory EE300 summer practice as a research intern in Communication Networks Research Group in Middle East Technical University, a leading technical university in Turkey. METU gives utmost importance to research and innovation with many of its members actively participating in research. In this ecosystem of reseach, I joined the research group of Prof. Elif Uysal, who was also my supervisor through the summer practice. Prof. Elif Uysal is a teaching professor in Middle East Technical University and the Principal Investigator of the Communication Networks Research Group. She conducts her research in communications area, especially Age of Information (AoI) in computer networks. In her research group, I have experienced the research atmosphere and learned many things regarding computer networks. I even had the opportunity to contribute to the literature. In the first three weeks of my practice, I mainly learned about the basics of the field, specifically, I was tasked to aid Orhan Yavaşcan in his papers work (Yavascan & Uysal, 2020). I performed simulations using MATLAB, then I implemented the findings of the simulations to the paper using LaTeX. Moreover, I did some minor corrections and checked the calculations. Then, in the remaining three weeks of my practice, I came up with a new policy which builds upon Orhan Yavaşcan's paper (Yavascan & Uysal, 2020). I made calculations, performed simulations using MATLAB, developed the idea, devised solutions and finally wrote the first draft of the paper using LaTeX.

In this report, I first describe the university. Then, I have given detalied explanation of my practice in two parts, first being the first three weeks and the second being the remaining two weeks, providing all the material. After that, in the "Conclusion" part, I give a brief summary of the report. Finally, I provide references.

2. DESCRIPTION OF THE INSTITUTION

2.1 Institution Name

Middle East Technical University

2.2 Institution Location

Orta Doğu Teknik Üniversitesi, Üniversiteler Mahallesi, Dumlupınar Bulvarı No:1 06800 Çankaya Ankara/TÜRKİYE

2.3 History of the Institution

Middle East Technical University was originally founded as "Orta Doğu Yüksek Teknoloji Enstitüsü" (Middle East High Technology Institute) on November 15th, 1956. It was intended to contribute to Turkey and other Middle Eastern countries in the need of skilled personnel in the natural and social sciences. On May 27th, 1959, METU was rendered a juridical entity with

the enactment of “Foundation Act No 7307”. Up until the year 1963, METU was consisting of two small parts, one in Kizilay’s Müdafaa Street that belonged to Social Security Office of Retirees and the other in the barracks behing the TBMM (Turkey’s National Grand Assembly). In 1963, METU was moved to its current campus, which is the first university campus of Turkey. Since its first foundation, METU is missioned with pioneering modern education in Turkey. Over the years, it brought so many innovations in many fields and continues to be one of the best universities in Turkey with its 41 undergraduate programs in 5 faculties.

2.4 Organization

METU has only grown over the years due to its high standarts of quality and pioneering academic education. Today, the university employs 791 faculty, 225 academic instructors and 1273 research assistants. Currently the university has around 28.000 students and the number of alumnis is over 120.000.

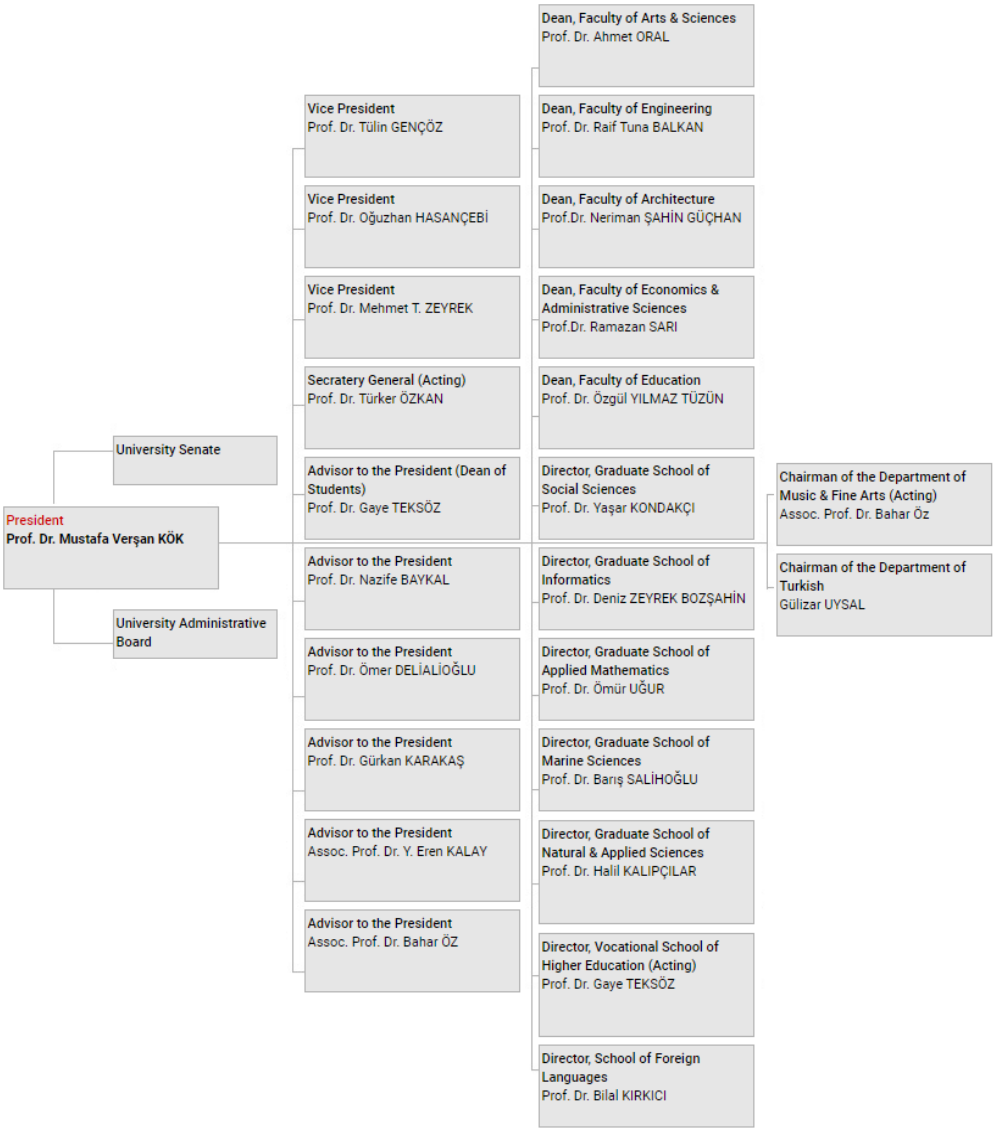

Figure 1: Organizational Structure of METU

2.5 METU EEE Computer Networks Research Group

I conducted my summer practice in the telecommunications lab of Electrical and Electronics Engineering Department, METU, as an undergradute researcher in the Computer Networks Research Group (METU CNG). Prof. Elif Uysal is the Principal Investigator of the group and she was also my supervisor thruoghout the summer practice. The main research area of METU CNG is Age of Information (AoI), a recently proposed metric for computer networks which is discussed elaborately in this report. More information can be found in METU CNG website http://cng.eee.metu.edu.tr/.

3. FIRST THREE WEEKS OF MY SUMMER PRACTICE

I started my practice in METU Electrical and Electronics Engineering department Telecommunications Lab on July 6th. In my first day, I met with my supervisor Prof. Elif Uysal and she gave me my first task. I was tasked to help Orhan Yavaşcan, one of Prof. Uysal's graduate students, about his paper "Analysis of Slotted ALOHA with an Age Threshold". His paper is about the analysis of Age of Information in random access channels, where the MAC layer protocol is an age threshold extension of slotted-ALOHA. In this first phase of my practice, I mainly learned about the field of computer networks and Age of Information. I started reading a textbook about computer networks in general. Moreover, I started reading the papers in the academic literature about Age of Information (Atabay, Uysal & Kaya, 2020; Maatouk, Assaad & Ephremides, 2019; Talak, Karaman & Modiano, 2018; Kaul et al., 2011). Let me first give some information about Age of Information and what we specifically worked on.

3.1 Age of Information

Computer networks have flourished significantly in the last few decades. With the integration of artifical intelligence, automation, Internet of Things and smart cities, a new page is opened to the approach of computer networks, since these applications require timeliness of information. For instance, in remote estimation, in order to keep the estimation error below a certain value, information should be updated regular enough to gather the freshest data possible. This requirement is not satisfied with the current means of networking, which means

there is a need for new policies and protocols in order to compensate. Age of Information (AoI) is a relatively new metric, which represents the time elapsed since the freshest information in the receiver side was generated. Due to its definition, AoI is a measure of how timely the information is delivered in the system. Since the mentioned areas of interest require time-sensitive information in order to perform properly, the average AoI of the system should be low enough. Current policies and protocols were proven to be inadequate, leading a way to papers of research on the subject over the years. What we were working on in my practice was a new MAC layer policy to reduce the average AoI in a multiple source single Access Point random access system. Traditionally a policy named slotted-ALOHA was applied in such systems.

3.1.1 Age of Information in Slotted-ALOHA Policy

In slotted-ALOHA policy, there are multiple senders and a single destination which we call the acess point. The time is slotted into frames of fixed length. At the beginning of each slot, sources either decide to send fresh information with a fixed probability or they stay idle. The sources who decide to attempt a transmission generate fresh data at the beginning of the slot and they send it through the common channel. Unless there is only one source sending data, collision occurs and all the packets are dropped. Since there is no contention resolution mechanism, the design parameters should be selected in a way to maximize the throughput. With the optimal selection of parameters, the maximum throughput achievable with the slotted-ALOHA policy is $1/e \approx 0.37$. In this configuration, it has been shown that the minimum AoI reachable is $en \approx 2.71n$, where n is the total number of sources (Yates & Kaul, 2017). This minimum achievable AoI level is not adequate for the modern applications mentioned, which leads way to the threshold-ALOHA policy that we have worked on during the first three weeks of my practice.

3.2 Threshold-ALOHA Policy

Threshold-ALOHA policy was first introduced as the Lazy Policy (Atabay, Uysal & Kaya, 2020). In this paper, the threshold-ALOHA policy is defined and simulated for small number of sources, but no open solution is given for the general case. Then, in Orhan's paper that we worked on, the policy is renamed as the threshold-ALOHA policy and it is analyzed in a complete manner. To be precise, the explicit steady state solution of the Markov Chain model established is derived. Then, using this steady state distribution, large network asymptotics are found and the general solution is completed (Yavascan & Uysal, 2020). What I have contributed to this paper through the first three weeks of my practice is that I first checked all the calculations in the paper, performed simulations on MATLAB and used LaTeX to integrate the findings to the paper either in words or as figures.

The main goal of threshold-ALOHA is to make slotted-ALOHA more AoI efficient. With this goal, an age threshold and a success feedback mechanism are implemented on top of the slotted-ALOHA. With the success feedback mechanism, the access point sends a 1-bit acknowledgement about a successfully delivered packet to the sender. With this mechanism employed, the sources can keep track of their ages, and with the age threshold employed, only those whose age exceeding the threshold become active sources. At the beginning of each slot, the decision of attempting a transmission is only made by active sources. This way, the competition for the channel utilization is only made between those sources that have the highest ages. This decreases the average AoI of the system while maintaining almost the same throughput levels with the slotted-ALOHA.

n is chosen as the total number of sources in the system model, while τ is the probability of attempt for an active source at the beginning of a time slot and Γ is the age threshold that is explained earlier. In order to analyze threshold-ALOHA, a Markov Chain is formed with ages of the sources, such that the states of the chain are *n* tuples which are constructed with the ages correspondingly. If a source did not transmit successfully in the previous time slot, its age just increments by 1, while it is set to 1 when it does transmit successfully. This Markov Chain is then truncated at Γ, making the state space a finite one. Then, it is shown that the steady state probability of a state solely depends on the number of active sources in it (i.e. the number of sources in the truncated states with the age state Γ). Using this information and the balance equations between the steady states, a general formulation is found that relates the steady state probability of all the states with *m* active sources, P_m, to the steady state probability of all the states with *m-1* active sources, P_{m-1}. This formulation is given as;

$$\frac{P_m}{P_{m-1}} = \frac{(1-(m-1)\tau(1-\tau)^{m-2})(n-m+1)}{\tau(1-\tau)^{m-1}m(\Gamma-1-n+m)}$$

With this result, the steady state distribution of the Markov Chain is found, since the steady state probabilities of the states are solely determined by the number of active sources, *m*. After this, the truncated Markov Chain is turned into a pivoted Markov Chain by arbitrarily selecting a source to be the pivot source. Then while the ages of all the other sources are still truncated at Γ, the pivot sources age is not truncated. Then, the system is analyzed through the ages of the pivot source. Since there is complete symmetry between the sources, this is done without loss of generality. While the other sources are truncatd at Γ, the pivot source is truncated at *s+1*, while its age is *s*. The ages of the pivot source are shown in Figure 2.

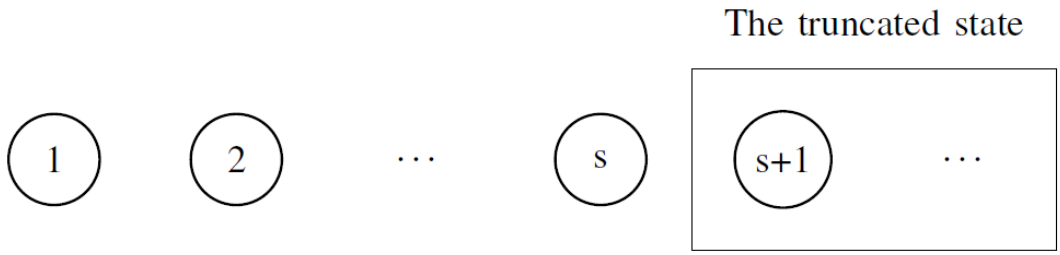

Figure 2: The Ages of the Pivot Source

After truncating the age of the pivot source at *s+1*, the total number of sources, *n*, is limited to infinity and then the system is anaylzed through the ages of the pivot source, which are also the states in the pivoted Markov Chain. The age state diagram of the pivot source is given in Figure 3.

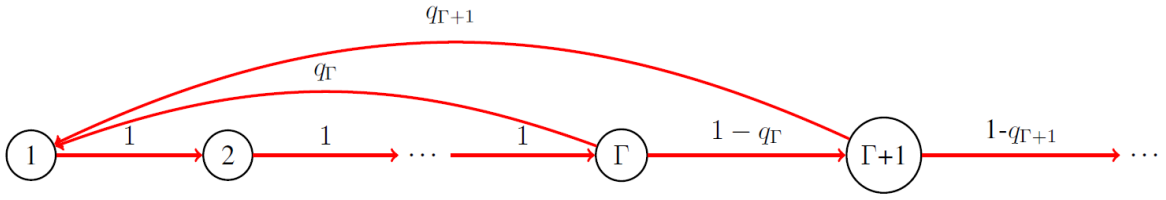

Figure 3: The State Diagram of the Pivot Source

It is shown that when the total number of sources, *n*, goes to infinity, the distribution of the number of active sources becomes independent from the individual sources (i.e. it converges to a value). In which case the transition probabilities in Figure 2 become fixed values and will be determined later in the analysis.

After the realization that the number of active sources, *m*, converges to a fixed value when $n \to \infty$, in order to analyze the limiting behaviour, the parameters of the system are scaled with *n* as follows;

$$\alpha = n\tau, \quad r = \Gamma/n, \quad k = m/n$$

In this scaling, the probability of transmission for the active sources, *τ*, is scaled with *n* and the parameter *α* is reached in the limiting case. Similarly, the parameter *r* is the scaled form of the age threshold *Γ*, while *k* is defined as the fraction of active users. Then, a function *f* is defined in the limiting case with our scales parameters as follows;

$$\lim_{n\to\infty} \ln \frac{P_m^{(s)}}{P_{m-1}^{(s)}} = \ln\left(\frac{e^{k\alpha}}{k\alpha} - 1\right) + \ln\left(\frac{r}{r+k-1} - 1\right) = f(k)$$

In the limit expression, *(s)* parts represent the cases where the states of the pivot source are both *s*. After the definition of the function *f*, it is shown that the decreasing roots of *f(k)* correspond one to one to the local maxima of P_m, with a scale of n. This is because of the definition of *f*, specifically the limit expression on the left side of the equation. Then, with this information, we can use the roots of *f(k)* in order to find the local maxima of P_m, which are the most likely values that *m* may have in the limiting case. An illustration of this relationship between *f(k)* and the pmf of *m* is given in Figures 4 and 5.

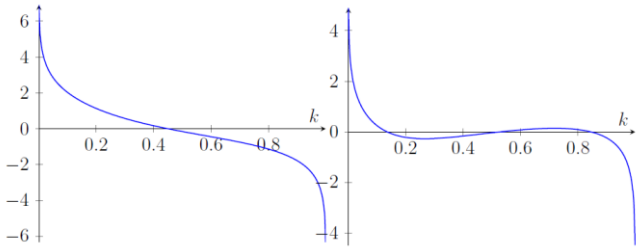

Figure 4: Two plots of *f(k)* for the parameters (*α*=2, *r*=1.5) (left plot) and (*α*=5, *r*=2.5) (right plot)

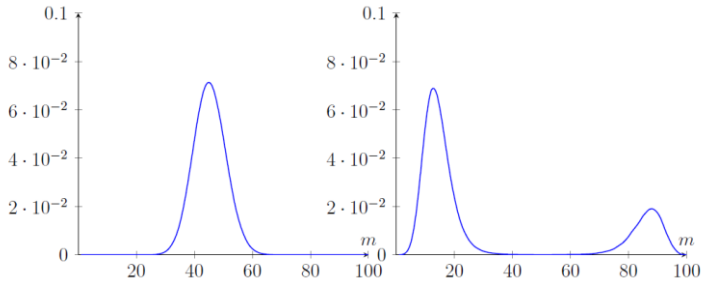

Figure 5: The pmf of *m* for the corresponding *f(k)* plots in Figure 4

Then, it is shown that when the total number of sources, *n*, goes to infinity, the fraction of active sources, *k*, converges to a fixed value, which means that the pmf of *m* concentrates at a point and becomes 1 at that point. When the point which *k* converges is analyzed, it is seen that it is one of the roots of *f(k)*. Afterwards, it is shown that *f(k)* has either 1 or 3 roots, and *k* converges to the only root in the first case and either the smallest or biggest root in the second case. The selection of parameters is what determines which case appears in the result.

Next, all cases are analyzed seperately. One root case is simple and straightforward but in the three roots case, it is desired to have *k* converge to the smallest root and an integral constraint is obtained for this purpose. Now that we know what value *k* converges for given parameters, the ages of the pivot source in the Pivoted Markov Chain discussed earlier is used to find the time average AoI expression in terms of the parameters of the system. Finally, the expression is minimized with optimal selection of parameters for both the cases for the roots of *f(k)* function. The results are given in Table 1.

	r	*α*	k_0	*AoI/n*	*Throughput*
Threshold-ALOHA (Single Root Case)	2.17	4.43	0.2052	1.4226	0.3658
Threshold-ALOHA (Three Roots Case)	2.21	4.69	0.1915	1.4169	0.3644
Slotted-ALOHA	0	1	1	$e \approx 2.7182$	$e^{-1} \approx 0.3678$

Table 1: The Optimal Parameters and the Resulting AoI and Throughput values for Thrsehold-ALOHA Cases and Slotted-ALOHA

As can be seen in Table 1, Threshold-ALOHA significantly reduces time average AoI compared to the Slotted-ALOHA policy. While achieving almost the half of the minimum time average AoI of slotted-ALOHA, Threshold-ALOHA also nearly maintains the throughput levels with only 1% decrease.

3.2.1 The MATLAB Code I wrote for the simulation of the Optimal Parameters of Threshold-ALOHA

```
n = 1000;
aaoimeanall=zeros(6,6);
for o=1:1:6
for p=1:1:6
alpha=4.5+(p-1)*0.1;
r=2+(o-1)*0.1;
tao = alpha/n;
theta = r*n;
attemptLimit = 1e+7;
n1=zeros(1,n);
for i = 1:n
    n1(i)=i;
end
curAge = floor(theta*rand(1,n));
aaoi = zeros(1,n);
pmf = zeros(1,n);
ageOfTransmission = zeros(1,n);
numberOfSourcesWhenTransmitted = zeros(1,n);
success = 0;
for t = 1:attemptLimit
    transmitting = 0;
    curSrc = -1;
    % find sources that can transmit
    for i = 1:n %source
        if(curAge(i)>=(theta-1))
            transmitting = transmitting + 1;
            tr_src(transmitting) = i;
```

```
        end
    end
    % find source that will successfully transmit
    if(transmitting >= 1)
        pmf(transmitting) = pmf(transmitting) + 1;
        q = tao*((1-tao)^(transmitting - 1));
        seed = rand(1,1);
        index = ceil(seed/q);
        if(transmitting >= index)
            curSrc = tr_src(index);
        end
    end
    % update current ages
    curAge = curAge + 1;
    if curSrc > -1
        success = success + 1;
        ageOfTransmission(success) = curAge(curSrc);
        numberOfSourcesWhenTransmitted(success) =
transmitting;
        curAge(curSrc) = 0;
    end
    % update average ages
    for i = 1:n
        aaoi(i) = ((t-1)*aaoi(i)+curAge(i))/t;
    end
end
aaoiMean = mean(aaoi);
pmf = pmf/attemptLimit;
[pmfMax,pmfPeak] = max(pmf/attemptLimit);
throughput = success/attemptLimit;
aaoimeanall(o,p)=aaoiMean;
end
end
```

What this code does is that it simulates the Threshold-ALOHA policy by applying the age threshold mechanism and than sweeps through different combinations of parameters. It records the resulting time average AoI into the `aaoimeanall` matrix in every iteration. Then we use the 'min' function of MATLAB in order to find the minimum possible AoI and with which parameter selections it is reached. This code confirms the theoretical results reached before. Furthermore, I used the pmf calculations in this code and plotted the pmf graphs in Figure 5 to be put in the paper.

3.2.2 The LaTeX code I wrote for the illustration in Figure 2

```
\begin{figure}[ht]
\centering
\begin{tikzpicture}
```

```
\begin{scope}[main node/.style={circle,thick,draw}]
   \node[main node,minimum size= 1 cm] (A) at (4,0) {1};
   \node[main node,minimum size= 1 cm] (B) at (6,0) {2};
   \node (C) at (8,0) {\ldots};
   \node[main node,minimum size= 1 cm] (D) at (10,0) {s};
   \node[main node] (E) at (12,0) {s+1};
   \node (F) at (14,0) {\ldots} ;
\end{scope}
\begin{scope}[every edge/.style={draw=red,very thick}]
   \draw (11,-1)  rectangle ++(4,2);
   \node (G) at (13,1.5) {The truncated state};
\end{scope}
\end{tikzpicture}
\caption{States of the pivot source in $\textbf{A}^{s,\Gamma}$ compared to $\textbf{P}^{\Gamma}$.}
\label{fig:augmented}
\end{figure}
```

This code draws the illustration for the states of the pivot source in the Pivoted Markov Chain, which can be seen in Figure 2.

3.2.3 The LaTeX code I wrote for the graph Ge^{-G} in the paper

```
\begin{figure}[b]
\centering
\begin{tikzpicture}
\begin{axis}[
samples=300,
xtick={0,1,2,3,4,5,6},
width=0.7\textwidth,
height=0.46\textwidth,
axis y line=left,
axis x line=middle,
xlabel=$G$,
]
\addplot[mark=none,color=blue,smooth,thick]gnuplot[domain=0:7]
{x*exp(-x)};
\draw [dashed,thin] (axis cs:1,0) – (axis cs:1,1/e);
\draw [dashed,thin] (axis cs:0.93,0) – (axis cs:0.93,0.359);
\node[color=black,scale=1,rotate=90] at (axis cs:0.72,0.15) {G=0.93};
\end{axis}
\end{tikzpicture}
\caption{Plot of $Ge^{-G}$}
\end{figure}
```

The aim of this code is to draw the graph in Figure 6, which measures the throughput optimality of our system in the AoI optimal operation. As can be seen in Figure 6, the throughput optimality is achieved at G=1 and AoI optimal selection of parameters results in the operating point G=0.89, very close to throughput optimal. G is a parameter obtained from the throughput expression in the limiting case.

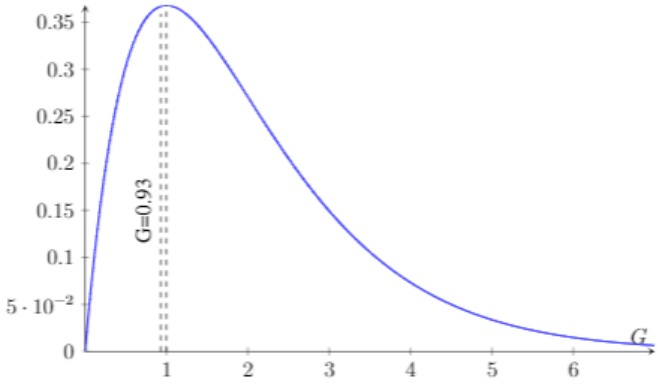

Figure 6: The Ge^{-G} graph that measures the throughput optimality in the limiting case

3.2.4 The LaTeX code I wrote for the illustration of the Aging Process

```
\begin{figure}[htbp]
\centering
\begin{tikzpicture}
\begin{axis}[
samples=300,
xtick={0,1,2,3,6},
xticklabels={0,1,2,3,$\ldots$},
ytick={0,1,2,3,4,5,6,7,8},
width=0.7\textwidth,
height=0.46\textwidth,
axis y line=left,
axis x line=middle,
xlabel=$t$,
ylabel=$AoI$,
ymin=0,
]
\addplot[mark=none,color=black,dotted,thick]gnuplot[domain=0:3]
{x+1};
\addplot[mark=none,color=black,dotted,thick]gnuplot[domain=3:8]
{x-2};
\addplot[mark=none,color=black,dotted,thick]gnuplot[domain=8:11]
{x-7};
\addplot[mark=none,color=black,dotted,thick]gnuplot[domain=11:12]
```

```
{x-10};
\addplot[mark=none,color=black,smooth,thick]gnuplot[domain=0:1]
{1};
\addplot[mark=none,color=black,smooth,thick]gnuplot[domain=1:2]
{2};
\addplot[mark=none,color=black,smooth,thick]gnuplot[domain=2:3]
{3};
\addplot[mark=none,color=black,smooth,thick]gnuplot[domain=3:4]
{1};
\addplot[mark=none,color=black,smooth,thick]gnuplot[domain=4:5]
{2};
\addplot[mark=none,color=black,smooth,thick]gnuplot[domain=5:6]
{3};
\addplot[mark=none,color=black,smooth,thick]gnuplot[domain=6:7]
{4};
\addplot[mark=none,color=black,smooth,thick]gnuplot[domain=7:8]
{5};
\addplot[mark=none,color=black,smooth,thick]gnuplot[domain=8:9]
{1};
\addplot[mark=none,color=black,smooth,thick]gnuplot[domain=9:10]
{2};
\addplot[mark=none,color=black,smooth,thick]gnuplot[domain=10:11]
{3};
\addplot[mark=none,color=black,smooth,thick]gnuplot[domain=11:12]
{1};
\draw [dotted,thick] (axis cs:3,4) -- (axis cs:3,3);
\draw [dotted,thick] (axis cs:8,7) -- (axis cs:8,1);
\draw [dotted,thick] (axis cs:11,4) -- (axis cs:11,1);
%\draw [dotted,thick] (axis cs:6,3) -- (axis cs:6,0);
\draw [thick] (axis cs:1,2) -- (axis cs:1,1);
\draw [thick] (axis cs:2,3) -- (axis cs:2,2);
\draw [thick] (axis cs:3,3) -- (axis cs:3,1);
\draw [thick] (axis cs:4,2) -- (axis cs:4,1);
\draw [thick] (axis cs:5,3) -- (axis cs:5,2);
\draw [thick] (axis cs:6,4) -- (axis cs:6,3);
\draw [thick] (axis cs:7,5) -- (axis cs:7,4);
\draw [thick] (axis cs:8,5) -- (axis cs:8,1);
\draw [thick] (axis cs:9,2) -- (axis cs:9,1);
\draw [thick] (axis cs:10,3) -- (axis cs:10,2);
\draw [thick] (axis cs:11,3) -- (axis cs:11,1);
\addplot[fill=white,only                                    marks,mark=*]
coordinates{(1,1)(2,2)(3,3)(4,1)(5,2)(6,3)(7,4)(8,5)(9,1)(10,2)(11,3)};
\addplot[only                                               marks,mark=*]
coordinates{(0,1)(1,2)(2,3)(3,1)(4,2)(5,3)(6,4)(7,5)(8,1)(9,2)(10,3)(11,1)};
```

\end{axis}
\end{tikzpicture}
\caption{Sample evolution curves for $\Delta_i(t)$ and $A_i(k)$ in time}
\end{figure}

What this code does is that it generates a plot of the aging process a source experiences in a time interval. This plot includes the evolution of both the discrete age function $A_i(k)$ and the continous age function $\Delta_i(t)$. The plot can be seen in Figure 7.

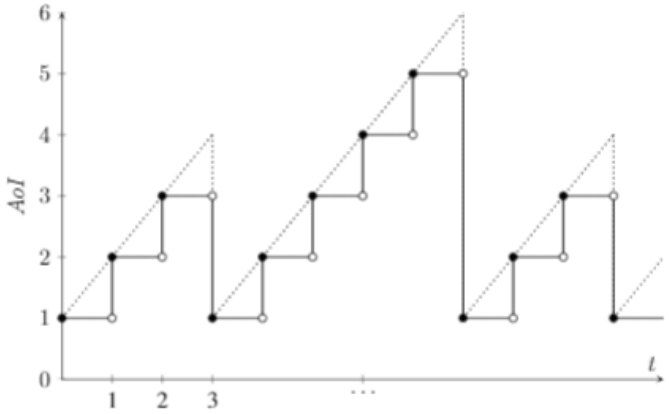

Figure 7: The Aging Process of a Source in a Time Interval

4. LAST TWO WEEKS OF MY SUMMER PRACTICE

After completing the work of Orhan's paper and submitting it, I came up with a modification of Threshold-ALOHA which I called Mini Slotted Threshold-ALOHA. Then I started to work on this idea by first simulating it in MATLAB and observing the results. The results of the simulations showed that the idea is worth writing a paper. Then I started the theoretical analysis with a similar approach used in Orhan's paper. Now, I will first give the MATLAB codes that I have written for the simulation, then I will provide the theoretical analysis of Mini Slotted Threshold-ALOHA.

4.1 The MATLAB code I wrote for the simulation of Mini Slotted Threshold-ALOHA

```
n = 1000;
r =1.59;
theta = r*n;
NumberofSlots = 1e+4;
ind_vector=zeros(1,1e+4);
indicator_of_situations=zeros(1,1e+4);
numofactive=zeros(1,1e+4);
curAge = floor(theta*rand(1,n));
ind=-1;
indicator_active=zeros(1,n);
indicator_attempter=zeros(1,n);
```

```
aaoi = zeros(1,n);
pmf = zeros(1,n);
success = 0;
zero_count=0;
one_count=0;
two_count=0;
alpha=10;
tao = alpha/n;
tao2 = 0.38;
for t = 1:NumberofSlots
    active=0;
 for i=1:n
     if(curAge(i)>=(theta-1))
         indicator_active(i)=1;
         active=active+1;
     end
 end
 if(active~=0)
 pmf(active)=pmf(active)+1;
 end
 for i=1:n
     if(indicator_active(i)==1)
         indicator_attempter(i)=rand(1,1)<tao;
     end
 end
 if(sum(indicator_attempter)==1)
     success=success+1;
     for i=1:n
         if(indicator_attempter(i)==1)
             ind=i;
         end
     end
 else
     ind=-1;
 end
 if(sum(indicator_attempter)>1)
     for i=1:n
         if(indicator_attempter(i)==1)
             indicator_attempter(i)=rand(1,1)<tao2;
         end
     end
   if(sum(indicator_attempter)==1)
     success=success+1;
     for i=1:n
         if(indicator_attempter(i)==1)
             ind=i;
         end
```

```
      end
    else
        ind=-1;
    end
  end
    if(sum(indicator_attempter)==0)
     indicator_of_situations(t)=0;
     zero_count=zero_count+1;
   else
       if(sum(indicator_attempter)==1)
     indicator_of_situations(t)=1;
     one_count=one_count+1;
   else
       if(sum(indicator_attempter)>1)
     indicator_of_situations(t)=2;
     two_count=two_count+1;
       end
       end
   end
  curAge=curAge+1;
  if(ind>0)
      curAge(ind)=0;
  end
  for i=1:n
      aaoi(i) = ((t-1)*aaoi(i)+curAge(i))/t;
  end
     ind_vector(t)=ind;
     for i=1:n
         indicator_active(i)=0;
     end
     for i=1:n
         indicator_attempter(i)=0;
     end
     numofactive(t)=active;
end
aaoiMean=mean(aaoi);
pmf = pmf/NumberofSlots;
throughput = success/NumberofSlots;
```

What this code does is that it simulates the Mini Slotted Threshold-ALOHA policy for 1000 sources and for 10^4 time slots. At every time slot, the system updates the system state of the Markov Chain model and calculates the time average AoI. The system model will be clearly explained in the theoretical analysis part.

4.2 The System Model Used for the Mini Slotted Threshold-ALOHA

Consider a wireless random-access channel with *n* sources and a single access point. The sources are intended to send time-sensitive data (temperature, velocity etc.) regularly to the access point using the shared channel. All nodes are synchronized to a slotted time frame. There is a success feedback mechanism in the system such that the AP sends a 1-bit acknowledgement to a source that successfully made a transmission in that slot. With this mechanism the sources are able to keep track of their ages. We use a *generate-at-will* model (Sun et al., 2017) in which there are no re-transmissions, sources generate a new packet when they attempt to transmit data in a slot. There can only be 1 successful transmission in a slot, hence there is no collision resolution mechanism.

We define $A_i[t]$ as the Age of Information (AoI) of source $i \in \{1, \dots, n\}$ at the time slot *t*. $A_i[t]$ is equal to the difference between the current time slot and the time-stamp of the freshest packet at the AP belonging to the source *i*. With our generate-at-will model assumption, this value is equal to the the number of slots that have passed since the latest successful transmission from source *i* plus 1. The success feedback mechanism informs the successful source to update its age to 1, otherwise the age increases by 1 at each slot. Correspondingly, the age process evolves as

$$A_i[t] = \begin{cases} 1, & \text{source } i \text{ transmits successfully at time slot } t-1 \\ A_i[t-1]+1, & \text{otherwise} \end{cases}$$

The average AoI of source *I* for a long period of time is defined as

$$\Delta_i = \lim_{T\to\infty} \frac{1}{T} \sum_{t=0}^{T-1} A_i[t]$$

where the limit exists.

4.3 The Mini Slotted Threshold-ALOHA Policy

In the analysis of threshold-ALOHA, a system age vector is constructed with ages of individual sources as

$$\mathbf{A}[t] \triangleq \langle A_1[t] \quad A_2[t] \quad \dots \quad A_n[t] \rangle$$

In Orhan's paper, it is shown that the evolution of this vector is a Markov Chain and that a truncated version of this Markov Chain is enough for age analysis purposes. In this finite state truncated Markov Chain, the source ages are truncated at *Γ* since the source's behaviour does not change after it becomes active. The truncated Markov Chain has a unique steady-

state distribution which is to be determined later in this part. Since the sources are symmetric and the Markov Chain is ergodic, the time average AoI can be found using the expression

$$\Delta_i = \lim_{t\to\infty} \mathbb{E}\left[A_i[t]\right]$$

4.3.1 The Slot Structure in Mini Slotted Threshold-ALOHA

In the analysis of both slotted ALOHA and threshold-ALOHA, the slots are homogeneous blocks of time which are sufficient for the transmission of a single data packet. What we add to this structure in the mini slotted threshold-ALOHA policy is that now slots consist of two parts, the mini slot and the data slot. The new structure can be seen in Figure 8.

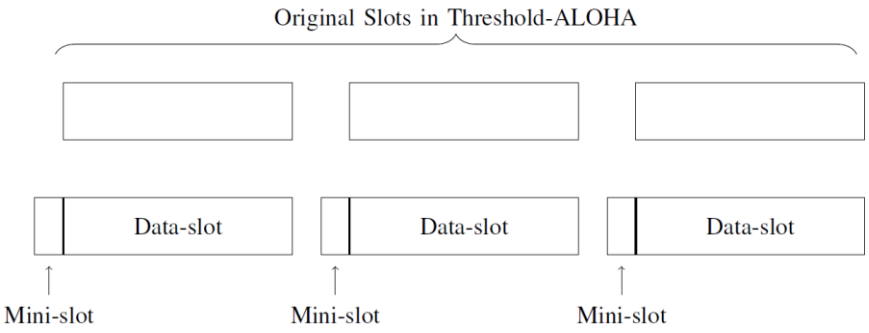

Figure 8: The Slot Structure of Mini Slotted Threshold-ALOHA

In threshold-ALOHA, all the active sources make a decision of becoming an attempter with probability τ at the beginning of each slot. Then the sources that become attempters start to send their data over the channel, resulting in a successful transmission only if there is no collision, in other words, only if they are the only source attempting a transmission. We refer to the decision making process at the beginning as a coin toss with probability τ of attempting. In mini slotted threshold-ALOHA, sources toss the coin once at the beginning of the mini-slot with probability τ, then unlike threshold-ALOHA, those who become attempters do not start to send the time-sensitive data right away, instead the attempters send just enough bits to make the AP recognise them (ID information). If the AP sends a success feedback to a source, then that source figures out that it is the only attempter and safely transmits its data in the data slot. However, if the attempting sources do not receive success feedback, this time they figure out that there are multiple attempters and there will be a collision. At this point, instead of sending their data anyways in the data slot, they toss the coin once again with a different probability τ_2. After the second toss, those who maintain their status of being an attempter send their data in the data slot. This gives the sources a second chance to come up with a sole attempter and save this slot that would be wasted with a collision in the threshold-ALOHA policy. This difference will prove to be beneficial in terms of both age and throughput. Nevertheless, the parameters and the lengths of the sub-slots need to be carefully selected to get optimal results. Next, we derive bounds for both the throughput and the average AoI.

4.3.2 An Upper bound for Throughput and A Lower bound for AoI

First, in order to find an upper bound for the throughput, we calculate probability of success for a time slot. As stated earlier, τ is the probability of becoming an attempter in the first toss and τ_2 is the probability of maintaining the status of being an attempter in the second toss. Let the number of active sources be m in the time slot and C_{MS} be the throughput of the mini-slotted threshold-ALOHA. Then the throughput of the mini slotted threshold-ALOHA is calculated as

$$C_{MS} = m\tau(1-\tau)^{m-1} + m\tau\tau_2[(1-\tau\tau_2)^{m-1} - (1-\tau)^{m-1}]$$

Then, in order to find the upper bound value, we asymptotically analyze this expression with large n. Let $G=m\tau$. The throughput expression in the limit of large n is

$$C_{MS} = \tau_2 G e^{-\tau_2 G} + (1-\tau_2) G e^{-G}$$

When this expression is analyzed, its maximum value is found to be 0.5315, which is the upper bound for the throughput. We can find a lower bound for the average AoI using the upper bound for the throughput (Chen et al., 2019).

Proposition 1. *The lower bound expression for the time average AoI is*

$$\frac{\Delta}{n} \geq \frac{1}{2C_{MS}} + \frac{1}{2n}$$

The proof for Proposition 1 can be found in the cited paper (Chen et al., 2019).

In our analysis, we consider the limit of large n, thus the second term goes to 0. Moreover, we found the maximum value of C_{MS} as 0.5315, then the lower bound for the average AoI is 0.9407.

4.3.3 The Steady States of the Markov Chain Model

In this part, we analyze the truncated Markov Chain that is formed with the evolution of the system age vector. Using the steady state probabilities of the recurrent states, we will derive the distribution of the number of active users, m, as done in Orhan's paper. First, we define the truncated system age vector as

$$\mathbf{A}^{\Gamma}[t] \triangleq \begin{pmatrix} A_1^{\Gamma}[t] & A_2^{\Gamma}[t] & \dots & A_n^{\Gamma}[t] \end{pmatrix}$$

where $A_i^{\Gamma}[t] \in \{1, \ldots, \Gamma\}$ is the AoI of source *i* at time $t \in \mathbb{Z}^+$ truncated at *Γ*. The $A_i^{\Gamma}[t]$ expression takes the value *Γ* if the source *i* is active in a slot (i.e. if its age is at least *Γ*), otherwise $A_i^{\Gamma}[t]$ takes the value of the sources age. Therefore, the $A_i^{\Gamma}[t]$ expression evolves as

$$A_i^{\Gamma}[t] = \begin{cases} 1, & \text{source } i \text{ updates at time } t-1, \\ \min\left\{A_i^{\Gamma}[t]+1,\ \Gamma\right\}, & \text{otherwise.} \end{cases}$$

$\{A^{\Gamma}[t], t \geq 1\}$ is a Markov Chain with a finite state space and a unique steady state distribution (Atabay, Uysal & Kaya, 2020). Now, we consider this Markov Chains recurrent class.

Proposition 2. *For distinct indices i and j, if a state* $\langle s_1\ s_2 \ldots s_n \rangle$ *in the truncated Markov Chain* $\{A^{\Gamma}[t], t \geq 1\}$ *is recurrent, then* $s_i = s_j$ *if and only if* $s_i = s_j = \Gamma$.

The proof of Proposition 2 can be found in Orhan's paper (Yavascan & Uysal, 2020).

What Proposition 2 essentially means is that states with two equal below-threshold ages are transient. Hence, in recurrent states the only repetitive age can be *Γ*. We will later prove that indeed all the states that satisfy Proposition 2 are recurrent. Furthermore, since there is a unique steady state distribution, all these recurrent states are in the same recurrent class. Next, in order to identify the recurrent states, we will define the *type* of a recurrent state as

$$T\langle s_1 \quad s_2 \quad \ldots \quad s_n \rangle = (M, \{u_1, u_2, \ldots, u_{n-M}\}),$$

In this notation, *M* is the number of active sources (i.e. the sources with the entry *Γ*), and the set $\{u_1, u_2, \ldots, u_{n-M}\}$ is the set of entries belonging to passive sources (i.e. sources with entry smaller than *Γ*). The reason to represent the active sources with their population rather than putting them one by one will be clear later.

Proposition 3. *Same type of states have equal steady state probabilities.*

Proof. Since the sources are symmetric, the ages below *Γ* in a state may belong to any passive source symmetrically. Then the total probability for these states are uniformly distributed.

In the next lemma, we discover the reason why we use the number of active users in our notation. We will prove that the steady state probability of a state is solely determined by the number of active users *M*, hence the set $\{u_1, u_2, \ldots, u_{n-M}\}$ has no effect on the steady state probability. Since our objective is to derive the distribution of the number of active users, this information will prove to be quite useful.

Lemma 1. *The following are valid for the truncated Markov Chain* $\{A^{\Gamma}[t], t \geq 1\}$:

i. M, which is the number of active sources given a state vector $\langle s_1\ s_2 \dots s_n \rangle$*, is what solely determines the steady state probability of the state vector.*

ii. Let P_m *be the total steady state probability of states with m active users. Then*

$$\frac{P_m}{P_{m-1}} = \frac{(1-(m-1)\tau(1-\tau)^{m-2} - (m-1)\tau\tau_2[(1-\tau\tau_2)^{m-2} - (1-\tau)^{m-2}])(n-m+1)}{(m\tau(1-\tau)^{m-1} + m\tau\tau_2[(1-\tau\tau_2)^{m-1} - (1-\tau)^{m-1}])(\Gamma - 1 - n + m)}$$

iii. The steady state probability of having no active sources is

$$P_0 = \frac{1}{1 + \sum_{m=1}^{n} \prod_{i=1}^{m} \frac{(1-(i-1)\tau(1-\tau)^{i-2} - (i-1)\tau\tau_2[(1-\tau\tau_2)^{i-2} - (1-\tau)^{i-2}])(n-i+1)}{(i\tau(1-\tau)^{i-1} + i\tau\tau_2[(1-\tau\tau_2)^{i-1} - (1-\tau)^{i-1}])(\Gamma - 1 - n + i)}}$$

Proof. For the proof of Lemma 1, we will define 4 types of state vectors. Let the type 1 be defined as $T_1 \triangleq (M, \{u_1, u_2, \dots, u_{n-M}\})$, where *M* is the number of active sources as before and the set $\{u_1, u_2, \dots, u_{n-M}\}$ contains no entry equal to 1. What this means is that there has not been a successful transmission in the previous slot. Note that there can be at most one entry equal to 1 in the recurrent states, which occurs in the case of successful transmission in the previous slot. Then, the previous slot can be one of two types, type 2 and type 3, defined as

- $T_2 \triangleq (M, \{u_1 - 1, u_2 - 1, \dots, u_{n-M} - 1\})$
- $T_3 \triangleq (M-1, \{\Gamma - 1, u_1 - 1, u_2 - 1, \dots, u_{n-M} - 1\})$

If there was no passive source with the age value *Γ-1* in the previous slot, then there must be *M* active slots in the previous slot, which is the case represented by type T_2. On the other hand, if there was a passive source with the age value *Γ-1* in the previous slot, then there must be *M-1* active slots in the previous slot since this passive source turns active in this slot, which is the case represented by type T_3. The fourth type is defined as $T_0 \triangleq (M-1, \{u_1, u_2, \dots, u_{n-M}, 1\})$ and it represents the case where the previous slot is one of the types T_2 and T_3 and it results with a successful transmission. This is why one of the values in the set $\{u_1, u_2, \dots, u_{n-M}, 1\}$ is equal to 1.

At this point, we see that if the previous slot is one of the types T_2 and T_3, then the present slot can be one of the two types T_0 and T_1. A type T_2 state precedes a type T_1 state with probability $1 - M\tau(1-\tau)^{M-1} - M\tau\tau_2[(1-\tau\tau_2)^{M-1} - (1-\tau)^{M-1}]$ and precedes a type T_0 state with probability $\tau(1-\tau)^{M-1} - \tau\tau_2[(1-\tau\tau_2)^{M-1} - (1-\tau)^{M-1}]$. A type T_3 state precedes a type T_1 state with probability $M(1-(M-1)\tau(1-\tau)^{M-2} - (M-1)\tau\tau_2[(1-\tau\tau_2)^{M-2} - (1-\tau)^{M-2}])$ and precedes a type T_0 state with probability $(M-1)\tau(1-\tau)^{M-2} - (M-1)\tau\tau_2[(1-\tau\tau_2)^{M-2} - (1-\tau)^{M-2}]$. If we define π_{T_i} to be the steady state probability of a state of type T_i, we can use the above arguments to write the following equations:

$$\begin{aligned}\pi_{\mathcal{T}_1} =&\pi_{\mathcal{T}_2}(1-M\tau(1-\tau)^{M-1}-M\tau\tau_2[(1-\tau\tau_2)^{M-1}-(1-\tau)^{M-1}])\\ &+\pi_{\mathcal{T}_3}M(1-(M-1)\tau(1-\tau)^{M-2}-(M-1)\tau\tau_2[(1-\tau\tau_2)^{M-2}-(1-\tau)^{M-2}])\\ \pi_{\mathcal{T}_0} =&\pi_{\mathcal{T}_2}\tau(1-\tau)^{M-1}+\tau\tau_2[(1-\tau\tau_2)^{M-1}-(1-\tau)^{M-1}]\\ &+\pi_{\mathcal{T}_3}(M-1)\tau(1-\tau)^{M-2}-(M-1)\tau\tau_2[(1-\tau\tau_2)^{M-2}-(1-\tau)^{M-2}]\end{aligned}$$

Since these equations represent all possible ways of transition between the recurrent states and since the truncated Markov Chain has a unique steady state distribution, this set of equations fully specifies the steady state probabilities. (*i*) part of the Lemma can be proven here by assigning the probability π_M to the states with *M* active sources. With this methodology, it is easy to see that $\pi_{T_1} = \pi_{T_2} = \pi_M$ and $\pi_{T_0} = \pi_{T_3} = \pi_{M-1}$. If we make the necessary substitutions, the first equation becomes:

$$\begin{aligned}\pi_M =&\pi_M(1-M\tau(1-\tau)^{M-1}-M\tau\tau_2[(1-\tau\tau_2)^{M-1}-(1-\tau)^{M-1}])\\ &+\pi_{M-1}M(1-(M-1)\tau(1-\tau)^{M-2}-(M-1)\tau\tau_2[(1-\tau\tau_2)^{M-2}-(1-\tau)^{M-2}])\end{aligned}$$

and the second equation becomes:

$$\begin{aligned}\pi_{M-1} =&\pi_M\tau(1-\tau)^{M-1}+\tau\tau_2[(1-\tau\tau_2)^{M-1}-(1-\tau)^{M-1}]\\ &+\pi_{M-1}(M-1)\tau(1-\tau)^{M-2}-(M-1)\tau\tau_2[(1-\tau\tau_2)^{M-2}-(1-\tau)^{M-2}]\end{aligned}$$

If we reduce these equations, they turn out to be the same equation that holds for all *m*, which is:

$$\frac{\pi_m}{\pi_{m-1}} = \frac{m(1-(m-1)\tau(1-\tau)^{m-2}-(m-1)\tau\tau_2[(1-\tau\tau_2)^{m-2}-(1-\tau)^{m-2}])}{m\tau(1-\tau)^{m-1}+m\tau\tau_2[(1-\tau\tau_2)^{m-1}-(1-\tau)^{m-1}]}.$$

Then, we have proven that part (*i*) holds. We will use this to find the total probability of having *m* active users in steady state. Due to Proposition 3, the total probability of having *m* active sources in steady state is the number of recurrent states with *m* active sources times the probability of one state with *m* active sources, which is π_m. The total number of recurrent states with *m* active sources is calculated as:

$$N_m = \binom{n}{m}\frac{(\Gamma-1)!}{(\Gamma-n-1+m)!}$$

Then, if we define P_m to be the total probability of having *m* active sources in steady state, we get:

$$P_m = N_m \pi_m$$

$$\frac{P_m}{P_{m-1}} = \frac{(1-(m-1)\tau(1-\tau)^{m-2} - (m-1)\tau\tau_2[(1-\tau\tau_2)^{m-2} - (1-\tau)^{m-2}])(n-m+1)}{(m\tau(1-\tau)^{m-1} + m\tau\tau_2[(1-\tau\tau_2)^{m-1} - (1-\tau)^{m-1}])(\Gamma-1-n+m)}$$

$$\sum_{m=0}^{N} P_m = 1$$

From these findings what we reach is:

$$P_0(1+\sum_{m=1}^{n}\prod_{i=1}^{m}\frac{(1-(i-1)\tau(1-\tau)^{i-2} - (i-1)\tau\tau_2[(1-\tau\tau_2)^{i-2} - (1-\tau)^{i-2}])(n-i+1)}{(i\tau(1-\tau)^{i-1} + i\tau\tau_2[(1-\tau\tau_2)^{i-1} - (1-\tau)^{i-1}])(\Gamma-1-n+i)} = 1$$

$$P_m = P_0\prod_{i=1}^{m}\frac{(1-(i-1)\tau(1-\tau)^{i-2} - (i-1)\tau\tau_2[(1-\tau\tau_2)^{i-2} - (1-\tau)^{i-2}])(n-i+1)}{(i\tau(1-\tau)^{i-1} + i\tau\tau_2[(1-\tau\tau_2)^{i-1} - (1-\tau)^{i-1}])(\Gamma-1-n+i)}$$

which gives the steady state distribution.

4.3.4 The Analysis of the Pivoted Markov Chain

In this part, we will arbitrarily choose a source to be our pivot source without loss of generality, since the sources are symmetric. We will analyze the system through the states of this pivot source by modifying the truncated Markov Chain in the previous subsection $\{A^{\Gamma}[t], t \geq 1\}$, and obtaining a *pivoted Markov Chain* $\{P^{\Gamma}[t], t \geq 1\}$. In this pivoted Markov Chain, all the source ages except the pivot source are truncated at *Γ*. As we did in the previous part, we will define the *type* of a state in the pivoted Markov Chain in order to extend the results of Lemma 1 as

$$\mathbf{T}^{\mathbf{P}}\langle S^{\mathbf{P}}\rangle \triangleq (s, M, \{u_1, u_2, \ldots, u_{n-M-1}\})$$

In this new notation, $s \in \mathbb{Z}^+$ is the state of the pivot source, *M* is the number of active sources (i.e. the sources with the entry *Γ*) excluding the pivot source, and the set $\{u_1, u_2, \ldots, u_{n-M}\}$ is the set of entries belonging to passive sources (i.e. sources with entry smaller than *Γ*), again excluding the pivot source. Similar to the truncated Markov Chain analysis, we will refer to such a state as *type M-state* where it is clear from the context.

Proposition 4.

i. P^{Γ} has a unique steady state distribution.

ii. A type m-state in P^{Γ} has a steady state probability equal to π_m, obeying the equations in the last part, given that $s \in \{1,2,\ldots,\Gamma-1\}$.

Proof. States in P^{Γ} where *s=1, 2, …, Γ-1* correspond to the states in the truncated Markov Chain A^{Γ} where the source selected as the pivot has the same age. The system visiting these corresponding states in P^{Γ} and A^{Γ} is merely the same event, therefore the steady state probabilities and the transition probabilities for these states are equal. Therefore, they follow the π_m/π_{m-1} expression in the previous part.

Now, for the states in P^{Γ} for which $s \geq \Gamma$, we will prove that steady state probabilities exist. In order to do this, we define a *augmented truncated Markov Chain* $\{A^{s,\Gamma}[t], t \geq 1\}$, in which the only difference with the pivoted Markov Chain is that now the pivot source is truncated at *s+1*. Truncation of the pivot source can be seen in Figure 2. At this point we consider the state where the state of the pivot source is *s+1* and the state of all the other sources are *Γ* in the augmented truncated Markov Chain $\{A^{s,\Gamma}[t], t \geq 1\}$. Then we realize that this specified state can be reached by any other state in the augmented truncated Markov Chain including itself, given that none of the last *s* consecutive time slots resulted in a successful transmission. This is an event with non-zero probability. Thus, there is a single recurrent class and a unique steady state distribution for the augmented truncated Markov Chain. Finally, since the states in the augmented truncated Markov Chain have one-to-one correspondence with the states in the pivoted Markov Chain, the existence of a unique steady state distribution for the augmented truncated Markov Chain proves the existence of a unique steady state distribution for the states in the pivoted Markov Chain.

Definition 1. *Let the type of a state in P^{Γ} be defined as $T^P\langle S^P\rangle = (s, m, \{u_1, u_2, \ldots, u_{n-M-1}\})$ where the $\{u_i\}$ are ordered from largest to smallest. Let Q(S^P), preceding type of S^P, be defined as follows:*

$$Q(S^{P}) = \begin{cases} T^{P}\langle S^{P}\rangle, & \text{if } s = 1 \\ (s-1, m, \{\Gamma - 1, u_1 - 1, u_2 - 1, \ldots, u_{n-m-2} - 1\}), & \text{if } s \neq 1, u_{n-m-1} = 1 \\ (s-1, m, \{u_1 - 1, u_2 - 1, \ldots, u_{n-m-1} - 1\}), & \text{if } s \neq 1, u_{n-m-1} \neq 1 \end{cases}$$

As can be seen from its definition, *Q(S^P)* is defined as the preceding type of S^P given that the number of active sources (excluding the pivot source), *m*, does not change. This reasoning does not hold for the case *s=1*, nonetheless, since this case is not particularly the point of interest, we choose *Q(S^P)* to be the same type with S^P. Now that we have covered all possibilities for *Q(S^P)*, we finally note that we will use *π(S^P)* or *π(s,m,{u_1, u_2, …, u_{n-m-1}})* to represent the steady state probability of S^P.

Lemma 2. *Choose two arbitrary states in P^{Γ}, S_1^P and S_2^P, where the state of the pivot source is equal for both states. Let the types of S_1^P and S_2^P be:*

$$T^{P}\langle S_1^{P}\rangle = \left(s, m_1, \{u_1, u_2, \ldots, u_{n-m_1-1}\}\right)$$

$$T^P\langle S_2^P\rangle = (s, m_2, \{u_1, u_2, \ldots, u_{n-m_2-1}\})$$

i. Let Q_1^P be any state satisfying $T^P\langle Q_1^P\rangle = Q(S_1^P)$. Then,

$$\lim_{n\to\infty} \frac{\pi(S_1^{\boldsymbol{P}})}{\pi(Q_1^{\boldsymbol{P}})} = 1$$

ii. If m_1=m_2, then.

$$\lim_{n\to\infty} \frac{\pi(S_1^{\boldsymbol{P}})}{\pi(S_2^{\boldsymbol{P}})} = 1$$

iii. If m_1=m_2+1, then

$$\lim_{n\to\infty} \frac{\pi(S_1^{\boldsymbol{P}})}{n\,\pi(S_2^{\boldsymbol{P}})} = \frac{1}{\alpha e^{-k\alpha} + \alpha\tau_2(e^{-\tau_2 k\alpha} - e^{-k\alpha})} - k$$

where $\lim_{n\to\infty} \frac{m_1}{n} = k$ and $\lim_{n\to\infty} \tau n = \alpha$. ($k, \alpha \in \mathbb{R}^+$)

Proof. See the Appendix.

Theorem 1. *For some $r, \alpha \in \mathbb{R}^+$ such that $\lim_{n\to\infty} \frac{\Gamma}{n} = r$ and $\lim_{n\to\infty} \tau n = \alpha$, define $f: (0.1) \to \mathbb{R}$:*

$$f(x) = \ln\left(\frac{1}{x\alpha e^{-x\alpha} + x\alpha\tau_2(e^{-\tau_2 x\alpha} - e^{-x\alpha})} - 1\right) + \ln\left(\frac{r}{x + r - 1} - 1\right)$$

Then, for all m such that $\lim_{n\to\infty} \frac{m}{n} = k \in (0,1)$ and $s \in \mathbb{Z}^+$

$$\lim_{n\to\infty} \ln \frac{P_m^{(s)}}{P_{m-1}^{(s)}} = f(k)$$

where $P_m^{(s)}$ is the steady state probability of having m active sources (excluding the pivot source), where the state of the pivot source is s.

Proof. The total steady state probability of the states with *m* active sources where the pivot source is in the state *s* is $P_m^{(s)}$. The total number of such states is given as:

$$N_m = \binom{n-1}{m} \frac{(\Gamma - 1)!}{(\Gamma - n + m)!}$$

Likewise, the total number of states with *m-1* active sources where the pivot source is in the state *s* is:

$$N_{m-1} = \binom{n-1}{m-1} \frac{(\Gamma-1)!}{(\Gamma-n+m-1)!}$$

Then, the following gives the desired result:

$$\begin{aligned}
\lim_{n\to\infty} \frac{P_m^{(s)}}{P_{m-1}^{(s)}} &= \lim_{n\to\infty} \frac{\sum_{i=1}^{N_m} \pi(S_i^{(m)})}{\sum_{j=1}^{N_{m-1}} \pi(S_j^{(m-1)})} \\
&\overset{(a)}{=} \lim_{n\to\infty} \frac{n\sum_{i=1}^{N_m} \left[\pi(S_i^{(m)})/n\pi(S_1^{(m-1)})\right]}{\sum_{j=1}^{N_{m-1}} \left[\pi(S_j^{(m-1)})/\pi(S_1^{(m-1)})\right]} \overset{(b)}{=} \lim_{n\to\infty} \frac{n\sum_{i=1}^{N_m} (\frac{1}{\alpha e^{-k\alpha}+\alpha\tau_2(e^{-\tau_2 k\alpha}-e^{-k\alpha})} - k)}{\sum_{j=1}^{N_{m-1}} 1} \\
&= \lim_{n\to\infty} \frac{nN_m(\frac{1}{\alpha e^{-k\alpha}+\alpha\tau_2(e^{-\tau_2 k\alpha}-e^{-k\alpha})} - k)}{N_{m-1}} \\
&= \lim_{n\to\infty} \frac{n(n-m)(\frac{1}{\alpha e^{-k\alpha}+\alpha\tau_2(e^{-\tau_2 k\alpha}-e^{-k\alpha})} - k)}{m(\Gamma-n+m)} \\
&= \left(\frac{1}{k\alpha e^{-k\alpha}+k\alpha\tau_2(e^{-\tau_2 k\alpha}-e^{-k\alpha})} - 1\right)\left(\frac{1-k}{r+k-1}\right)
\end{aligned}$$

where in the (a) step both sides of the fraction are divided to the steady state probability of a state with *m-1* active sources where the pivot source is in the state *s*, and (b) follows from Lemma 2 (ii) and (iii). Hence,

$$\lim_{n\to\infty} \ln \frac{P_m^{(s)}}{P_{m-1}^{(s)}} = \ln(\frac{1}{k\alpha e^{-k\alpha}+k\alpha\tau_2(e^{-\tau_2 k\alpha}-e^{-k\alpha})} - 1) + \ln(\frac{r}{r+k-1} - 1) = f(k)$$

What we essentially discovered is that as$n \to \infty$, the relation $P_m^{(s)}/P_{m-1}^{(s)}$ solely determines the distribution of *m*, no matter what the *s* value is. This means that the number of active sources excluding the pivot source, *m*, is independent of the state of the pivot source. This result is formally expressed in the following corollary:

Corollary 1. *In the limit of a large network ($n \to \infty$),*

i. The number of active sources, m, (excluding the pivot) and the state of the pivot source, s, are independent.

ii. Given that the pivot source is active (i.e.$s \geq \Gamma$), $\tau(1-\tau)^{m-1} + \tau\tau_2[(1-\tau\tau_2)^{m-1} - (1-\tau)^{m-1}]$ is the probability of a successful transmission being made by the pivot source which has no dependence on s.

iii. The probability of the pivot state being reset to 1 given that the pivot is active is $q_s = \lim_{l\to\infty} \sum_{m=0}^{l} P_m^{(s)} \left(\tau(1-\tau)^{m-1} + \tau\tau_2[(1-\tau\tau_2)^{m-1} - (1-\tau)^{m-1}]\right)$.

Proof. Parts (i) and (ii) follow from the proof of Lemma 1. Since the distribution of the number of active sources *m* and the state of the active source *s* are independent, no mater what the *s* value is, the pivot source observes the same number of active sources. Hence, the transition probabilities from $s = i$ to $s = i + 1$ for $i < \Gamma$ and, and the transition probability from $s \geq \Gamma$ to 1 depends only on the number of active users. This means the evolution of the pivot source state *s* is like shown in Figure 3.

The transitions to the state 1 in Figure 3 represent successful transmissions made by the pivot source. In the rest, we will consider the asymptotic case of a large network as *n* grows. All the transition probabilities to 1 (i.e. all the successful transitions of the pivot source) will have the same probability q_0 when $(n \to \infty)$, which will be showed later.

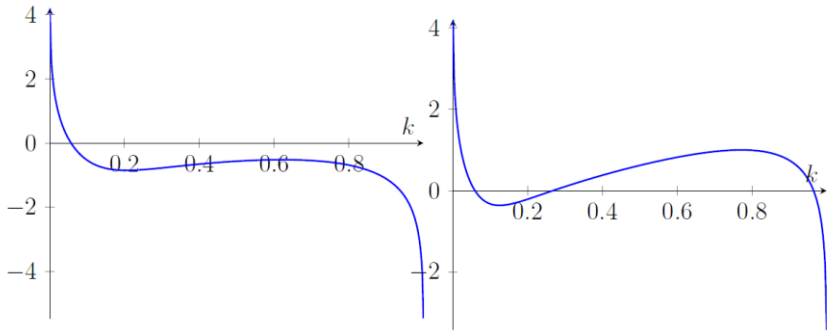

Figure 9: Two plots of *f(k)* for the parameters (*α*=6, *r*=2.5, τ₂=0.38) (left) and (*α*=15, *r*=2, τ₂=0.40) (right)

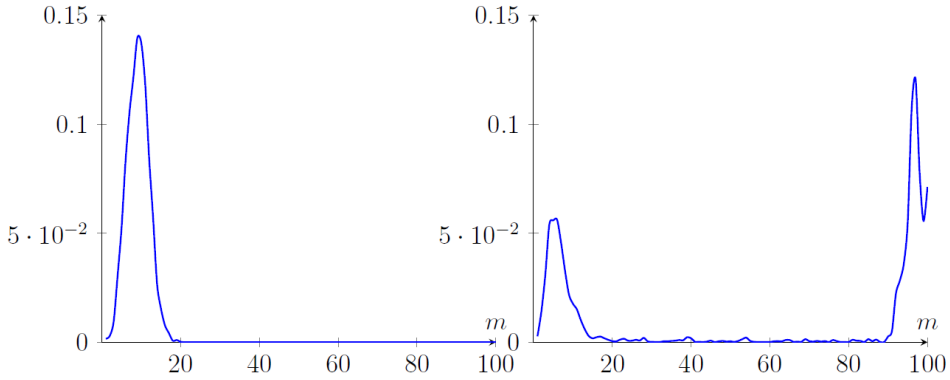

Figure 10: The pmf of *m* for the corresponding *f(k)* plots in Figure 9

4.3.5 Large Network Asymptotics

In this subsection, we will examine the asymptotic behaviour of the number of active sources *m* and find its PMF when $(n \to \infty)$. We will investigate the properties of the function *f* of Theorem 1, since it provides valuable insight on the distribution of *m*. With this

methodology, we will prove that the fraction of active sources, *k*, converges to the root of *f* in probability, which will be presented in Theorem 2.

We will replace some parameters of the model, τ and Γ, in order to make the asymptotic analysis in the network size *n* easier. Instead of these parameters, we will use the following ones which control their scaling with *n*. Due to its definition, the fraction of active users, *k*, will take values between 0 and 1.

$$\alpha = n\tau, \quad r = \Gamma/n, \quad k = m/n$$

Proposition 5. *The local maxima of P_m correspond one-to-one to roots of f where f is decreasing, with a scale of n.*

In this part, we assign α, *r* and τ_2 to be fixed system parameters while *k* is variable, and it varies with the instantaneous system load. Due to its definition, *f(k)* determines the change in P_m in a way that the roots of *f(k)* correspond to local extrema of P_m. When both $\ln P_m/P_{m-1}$ and $\ln P_m/P_{m+1}$ are positive at a point then it is a local maxima of P_m, which corresponds to decreasing roots of *f(k)*.

In this paper, we analyze two cases for the roots of *f(k)*, one root case and three root case, which correspond to one local maximum and two local maxima for P_m, respectively. Other cases with more roots of f(k) were observed to perform poorly in terms of AoI in our simulations. Although they show similar properties, one local maximum and two local maxima cases are analyzed seperately. Theorem 2 analyzes the one local maximum case where *f(k)* has only one root. Two local maxima case will be discussed in the next subsection.

Theorem 2. *Let m be the number of active sources and k_0 be the only root of f(k). For the sequence $\varepsilon_n = cn^{-1/3}$ where $c \in \mathbb{R}^+$,*

$$Pr\left(\left|\frac{m}{n} - k_0\right| < \varepsilon_n\right) \to 1$$

The proof of Theorem 2 can be found in Orhan's paper (Yavascan & Uysal, 2020).

What this theorem essentially means is that the fraction of active sources *k* converges to a value k_0, as the network size gets large (i.e. $n \to \infty$). Loosely speaking, the mini slotted threshold-ALOHA policy acts like the regular slotted-ALOHA policy with fewer number of active sources, nk_0, in the limit of large network size. Since nk_0 sources will be active in a time slot while the rest of the sources stay passive, the system resembles the slotted-ALOHA with nk_0 sources in total. In this large network conditions, both the throughput and the average age will be significantly improved with optimal selection of parameters, as will be shown later in this section.

4.3.6 Two Local Maxima Case

Before presenting the results for throughput and average AoI, we analyze the two local maxima case of the previous subsection here. Theorem 3 very much resembles Theorem 2; however, it has an additional integral constraint to be applicable.

As already explained in the previous section, roots of *f(k)* where *f* is decreasing correspond one-to-one with the peaks of the probability distribution of *m*. In the context of this subsection, there are two such roots, thus, two possible values the number of active sources *m* may converge to in probability. With the goal of analyzing this system, we define the following state sets:

$$\mathcal{S}_0 \triangleq \left\{ S \mid T\langle S \rangle = (m, \{u_1, u_2, \ldots, u_{n-m}\}) \text{ where } \frac{m}{n} \leq \frac{k_0 + k_1}{2} \right\}$$

$$\mathcal{S}_1 \triangleq \left\{ S \mid T\langle S \rangle = (m, \{u_1, u_2, \ldots, u_{n-m}\}) \text{ where } \frac{k_0 + k_1}{2} < \frac{m}{n} < \frac{k_1 + k_2}{2} \right\}$$

$$\mathcal{S}_2 \triangleq \left\{ S \mid T\langle S \rangle = (m, \{u_1, u_2, \ldots, u_{n-m}\}) \text{ where } \frac{k_1 + k_2}{2} \leq \frac{m}{n} \right\}$$

In these set definitions, mid-points between three roots are chosen as boundaries and three regions are formed. The region around the smaller root is defined as the set S_0, while the region around the larger root is defined as the set S_2. The region that lies between is defined as the set S_1. The sets can be seen in Figure 11.

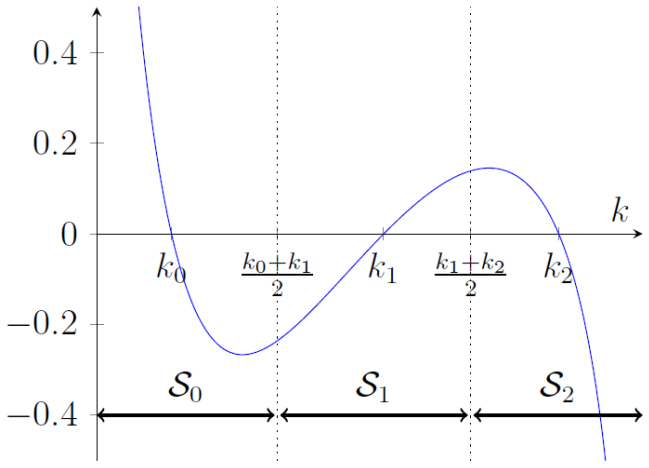

Figure 11: State Sets

Given that the integral of *f(k)* from the smaller root to the larger root is negative, the probability of the state sets S_1 and S_2 decay to 0 as $n \to \infty$, as shown in Theorem 3. Hence, when the probability of the state set S_0 becomes 1, the principles used for the single root case are used to find similar results.

Theorem 3. *Let k_0, k_1 and k_2 be three distinct roots of f(k) in increasing order and m be the number of active sources.*

i. If

$$\int_{k_0}^{k_2} f(k)dk \ < 0$$

then for the sequence $\varepsilon_n = cn^{-1/3}$ where $c \in \mathbb{R}^+$,

$$Pr(\left|\frac{m}{n} - k_0\right| < \ \varepsilon_n) \to 1$$

ii. If

$$\int_{k_0}^{k_2} f(k)dk \ > 0$$

then for the sequence $\varepsilon_n = cn^{-1/3}$ where $c \in \mathbb{R}^+$,

$$Pr(\left|\frac{m}{n} - k_2\right| < \ \varepsilon_n) \to 1$$

The proof of Theorem 2 can be found in Orhan's paper (Yavascan & Uysal, 2020).

Depending on the sign of the integral, the ratio of active users, *k*, converges to either k_0 or k_2. The desired case is the integral result being negative, since otherwise *k* converges to the larger root, which means more active sources at a time slot. Therefore, system parameters should be carefully selected in order to ensure that the integral result is negative, and *k* converges to the value k_0.

Although the two local maxima case yields similar results with the single local maximum case, there are some drawbacks regarding the former. In networks with fewer number of users, steady state probabilities of the state sets S_1 and S_2 may not get small enough to yield the desired results. As these states have more active sources, this situation results in congestions in the channel due to frequent collisions. Consequently, the benefits of our policy require that this case is avoided. Single root case does not have this drawback and approaches the theoretical value more quickly.

Another problem that may arise in the two local maxima case is that in networks with large number of users, poor selection of initial conditions may lead to undesired results. If all the sources are initially active, the aforementioned congestion scenarios occur, making the convergence in Theorem 3 impossible in a reasonable time. Moreover, if the initial state of the system is in the state set S_2, it may again not be able to reach the state set S_0 in a

reasonable time. In order to avoid such problems, the initial states of the sources may be randomly selected.

Although it has some drawbacks to be careful about, the two local maxima case provides asymptotically optimal results and it is preferable for large networks.

4.3.7 Steady State Time Average AoI in the Large Network Limit

Theorem 4. *In the large network limit (i.e. $n \to \infty$), optimal parameters of the mini slotted threshold-ALOHA satisfy the following:*

$$\lim_{n\to\infty} \frac{\Gamma^*}{n} = 1.59$$

$$\lim_{n\to\infty} n\tau^* = 10$$

$$\tau_2^* = 0.38$$

Furthermore, the optimal expected AoI at steady state scales with n as:

$$\lim_{n\to\infty} \frac{\Delta^*}{n} = 0.9641$$

Proof. At the ending of part 4.3.4, q_0 was defined as the successful transmission probability of an active source, moreover, it has been argued that this value is fixed, or independent of age, in the steady state as the number of active sources converge to a value. We can also express q_0 in the following way:

$$q_0 = \mathbb{E}[\tau(1-\tau)^{M-1} + \tau\tau_2[(1-\tau\tau_2)^{M-1} - (1-\tau)^{M-1}]]$$

where the expectation is over the PMF of the number of active sources, *M*, at steady state, which was analyzed earlier. We will first prove that

$$\lim_{n\to\infty} n\, q_0 = \alpha e^{-k_0\alpha} + \alpha\tau_2(e^{-\tau_2 k_0\alpha} - e^{-k_0\alpha})$$

Let γ_n be defined as:

$$\gamma_n \triangleq \Pr(m_0 - cn^{2/3} < M < m_0 + cn^{2/3})$$

where $m_0 = nk_0$. From Theorems 2 and 3, $\gamma_n \to 1$ as $n \to \infty$. When *M* satisfies the bounds given in the definition of γ_n, the successful transmission probability, q_0, is also bounded. With this information, the following bound on q_0 is found:

$$\gamma_n[(\tau(1-\tau)^{m_0}+\tau\tau_2[(1-\tau\tau_2)^{m_0}-(1-\tau)^{m_0}])(1-\tau)^{-cn^{2/3}}]<q_0$$

$$q_0<\gamma_n[(\tau(1-\tau)^{m_0}+\tau\tau_2[(1-\tau\tau_2)^{m_0}-(1-\tau)^{m_0}])(1-\tau)^{cn^{2/3}}]+(1-\gamma_n)$$

As $n\to\infty$, both upper and lower bounds converge to $\tau(1-\tau)^{m_0}+\tau\tau_2[(1-\tau\tau_2)^{m_0}-(1-\tau)^{m_0}]$. Finally,

$$\lim_{n\to\infty} n\,q_0=\lim_{n\to\infty} n\tau(1-\tau)^{m_0}+n\tau\tau_2[(1-\tau\tau_2)^{m_0}-(1-\tau)^{m_0}]=\alpha e^{-k_0\alpha}+\alpha\tau_2(e^{-\tau_2 k_0\alpha}-e^{-k_0\alpha})$$

Since the transitions between the states of a source is as given in Figure 3, value of q_0 can be used to compute the steady state probabilities of the states. Furthermore, the states correspond one-to-one with the ages the source have. Then, finding the steady state probabilities of the states is merely finding the steady state probabilities of the ages. With this methodology, the steady state probability of state *j* is:

$$\pi_j=\frac{(1-q_0)^{max\{j-\Gamma,0\}}}{\Gamma-1+1/q_0},\qquad j=1,2,\dots$$

The expected time average AoI expression is found using the steady state probabilities of the ages:

$$\Delta=\frac{\Gamma(\Gamma-1)}{2(\Gamma-1+1/q_0)}+1/q_0$$

The average AoI is also expressed in the limit of large network as:

$$\lim_{n\to\infty}\frac{\Delta}{n}=\frac{r^2}{2(r+\frac{1}{\alpha e^{-k_0\alpha}+\alpha\tau_2(e^{-\tau_2 k_0\alpha}-e^{-k_0\alpha})})}+\frac{1}{\alpha e^{-k_0\alpha}+\alpha\tau_2(e^{-\tau_2 k_0\alpha}-e^{-k_0\alpha})}$$

The system parameters *r* and k_0 can be used to re-express the age expression as:

$$\lim_{n\to\infty}\frac{\Delta}{n}=r\frac{k_0^2+1}{2(1-k_0)}$$

With the right selection of system parameters, the Average AoI expression can be minimized.

Analyzing the age expression, optimal parameters and some other steady-state characteristics such as k_0 and AAoI, are derived for mini slotted threshold-ALOHA. These findings are provided in Table 2 with corresponding values for threshold-ALOHA and slotted-ALOHA for comparison. Since both threshold-ALOHA and mini slotted threshold-ALOHA have two regimes of operation, namely two local maxima case and single local maximum case, the results for these regimes are provided seperately.

	r^*	α^*	τ_2^*	k_0^*	Δ^*/n	Throughput
Mini Slotted Threshold-ALOHA (single local maximum)	1.59	9.8	0.37	0.1565	0.9656	0.5252
Mini Slotted Threshold-ALOHA (double local maxima)	1.59	10	0.38	0.1555	**0.9641**	0.5266
Threshold-ALOHA (single local maximum)	2.17	4.43	-	0.2052	1.4226	0.3658
Threshold-ALOHA (double local maxima)	2.21	4.69	-	0.1915	**1.4169**	0.3644
Slotted-ALOHA	0	1	-	1	e	e^{-1}

Table 2: A comparison of optimized parameters of ordinary slotted ALOHA, threshold-ALOHA and mini slotted threshold-ALOHA and the resulting AoI and throughput values. r^*: age-threshold/n; τ_2^*: probability of transmission in the second toss; α^*: transmission probability × n; k_0^*: expected fraction of active users; Δ^*: avg. AoI

The optimal AoI expression for the slotted-ALOHA is (Yates & Kaul, 2017):

$$\Delta = \frac{1}{2} + \frac{1}{\tau(1-\tau)^{n-1}}$$

In this expression, τ is chosen to be $1/n$ in order to obtain the smallest AoI value. The following limit gives the optimal AoI under slotted-ALOHA (Munari & Frovlov, 2020):

$$\lim_{n\to\infty} \frac{\Delta^{SA}}{n} = \lim_{n\to\infty} \frac{1}{2n} + \frac{1}{\left(1-\frac{1}{n}\right)^{n-1}} = e$$

As presented in Table 2, the average AoI value drops to nearly half this value in threshold-ALOHA policy, while approximately maintaining the throughput level of slotted-ALOHA. Mini slotted threshold-ALOHA policy we propose in this paper, on the other hand, significantly increases the throughput value and decreases the average AoI to an even smaller value.

4.3.8 Spectral Efficiency of Mini Slotted Threshold-ALOHA

Before starting the numerical analysis, we analyze the spectral efficiency of the mini slotted threshold-ALOHA policy in this subsection. Since we add a mini slot to the slots of

threshold-ALOHA, the loss in spectral efficiency becomes a concern. There is no loss of spectral efficiency if the extra time the system spends in the mini slot is compensated with the increase in the throughput. We will show that the mini slotted threshold-ALOHA not only preserves the spectral efficiency but also probably increases it.

η	*Spectral efficiency of the threshold-ALOHA (bits/s/Hz)*
η'	*Spectral efficiency of the mini slotted threshold-ALOHA (bits/s/Hz)*
B	*Channel Bandwidth*
H	*Time Horizon*
T_b	*The time it takes to send 1 bit (s)*
Θ_1	*Throughput of threshold-ALOHA*
Θ_2	*Throughput of mini slotted threshold-ALOHA*
c	*Number of bits in the data slot*
d	*Number of bits in the mini slot*

Table 3: Notation table for the symbols relating to spectral analysis

With the definitions given, we first derive the following expressions.

$$\eta = \frac{H\theta_1 c}{HBcT_b} = \frac{\theta_1}{BT_b}$$

$$\eta' = \frac{H\theta_2 c}{HB(c+d)T_b} = \frac{\theta_2 c}{(c+d)BT_b}$$

$$\frac{\eta'}{\eta} = \frac{\theta_2}{\theta_1}\frac{c}{c+d}$$

In order to preserve the spectral efficiency, the η / η' expression should at least be equal to 1. The typical values the $\Theta_2/\ \Theta_1$ expression takes are given in Table 4.

	Mini Slotted Threshold-ALOHA (Θ_2)	Threshold-ALOHA (Θ_1)	$\Theta_2/\ \Theta_1$
1000 Sources	0.5251	0.3632	1.448
500 Sources	0.5179	0.3581	1.446
100 Sources	0.5019	0.3633	1.382

Table 4: Typical values the $\Theta_2/\ \Theta_1$ expression takes for three different *n* values, for both the mini slotted threshold-ALOHA and threshold-ALOHA

With the typical values of $\Theta_2/\ \Theta_1$ given in Table 4, we see that as long as the *c/d* expression is greater than 2.23, there is no loss of spectral efficiency in mini slotted threshold-ALOHA policy.

The typical value for *c* is around 1.5-2 kbytes in real time systems such as IEEE 802.11. On the other hand, a *d* value of 128 bits is sufficient for the purposes of the mini slot since only the ID information of sources is needed. Then, the *c/d* expression is much greater than

2.23, which means the mini slots does not decrease the spectral efficiency of the system. In fact, the mini slotted threshold-ALOHA has a greater spectral efficiency than threshold-ALOHA in all practical cases.

4.3.9 Numerical Results and Discussion

In this part, we will provide numerical analysis with simulation results and we will make comparisons with slotted-ALOHA and threshold-ALOHA. In Figure 12 and Figure 13, the comparison is made for both the optimal average AoI and the throughput. Both the optimal average AoI and the throughput values are plotted against *n*, the total number of sources, as *n* ranges from 50 to 1000. In the simulations, the system runs for 10^7 time slots. Initial states of sources are randomized in order to prevent undesired congestion scenarios and to ensure the distributed nature of the system is preserved. Note that while threshold-ALOHA achieves nearly the half age of slotted-ALOHA, the mini slotted threshold-ALOHA achieves roughly one third of the age of slotted-ALOHA.

If we compare threshold-ALOHA and mini slotted threshold-ALOHA, the first and foremost difference is the optimal average AoI value. As already discussed in 4.3.5, the mini slotted threshold-ALOHA policy cuts the number of active sources in a time slot to *15%* of all sources in the system, while for the threshold-ALOHA this value is *20%*. Mini slotted threshold-ALOHA reduces the optimal average AoI of the threshold-ALOHA by *32%*, while it increases the throughput value by *45%* and almost guarantees to increase the spectral efficiency.

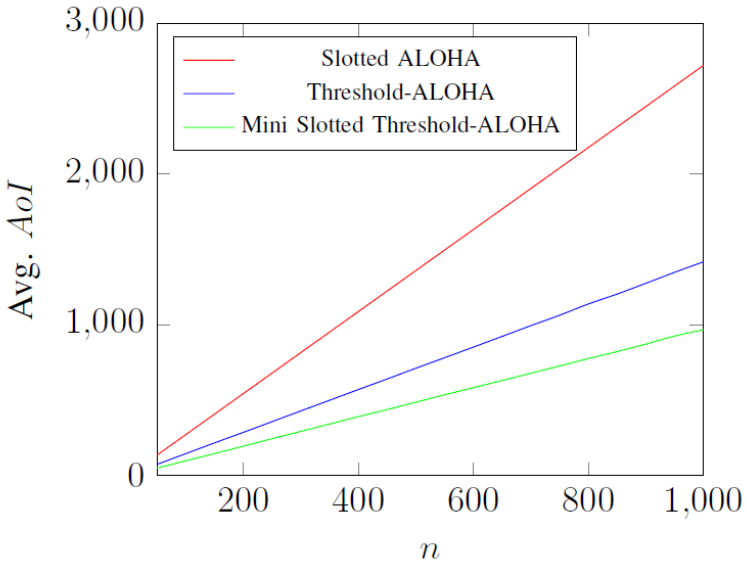

Figure 12: Optimal *time average AoI* vs *n*, number of sources, under Slotted ALOHA (computed), threshold-ALOHA (simulated) and mini slotted threshold-ALOHA (simulated).

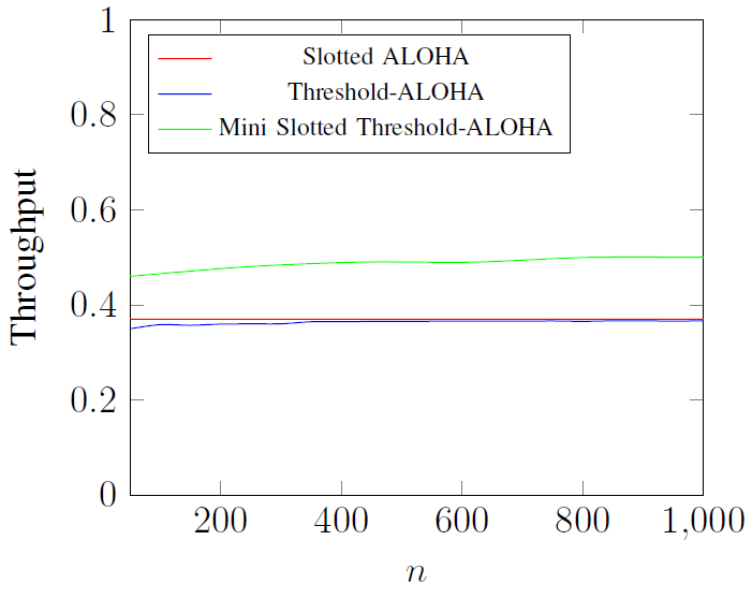

Figure 13: Throughput vs *n*, number of sources, under Slotted ALOHA (computed from expression), threshold-ALOHA (simulated) and mini slotted threshold-ALOHA (simulated).

5. CONCLUSION

In this report, I have provided information about my research summer practice in METU. I first detailed the work I have done in the first three weeks of my practice, where I mainly learned about the subject and assisted Orhan Yavaşcan in his paper's work. I provided codes I have written and figures that I have plotted in this phase. Then, in the last two weeks of my practice, I camee up with my own idea for a new policy in MAC layer with the aim of AoI minimization. Then, I provided detailed analysis of this policy that I named as mini slotted threshold-ALOHA. During my summer practice, I have gained a lot of experience and information by directly making research or providing assistance. I had the opportunity to get inside the academic research environment, which I found quite challenging and amusing at the same time.

6. REFERENCES

A. Maatouk, M. Assaad and A. Ephremides, "Minimizing the age of information in a csma environment" *arXiv preprint arxiv: 1901.00481,* 2019.

D. C. Atabay, E. Uysal and O. Kaya, "Improving age of information in random access channels" in *Proc. AoI Workshop in conj. with IEEE INFOCOM*, July 2020.

O. T. Yavascan, E. Uysal "Analysis of slotted-ALOHA with an age threshold" *arXiv preprint arxiv: 2007.09197*, 2020.

R. D. Yates and S. K. Kaul, "Status updates over unreliable multiaccess channels" in *2017 IEEE International Symposium on Information Theory (ISIT)*, pp. 331-335, IEEE, 2017.

R. Talak, S. Karaman and E. Modiano, “Distributed scheduling algorithms for optimizing information freshness in wireless networks” in *2018 IEEE 19. International Workshop on Signal Proccessing Advances in Wireless Communications (SPAWC)*, pp. 1-5, IEEE, 2018.

S. K. Kaul, M. Gruteser, V. Rai and J. Kenney, “Minimizing age of information in vehicular networks” in *2011 8. Annual IEEE Communications Society Conference on Sensor, Mesh and Ad Hoc Communications and Networks*, IEEE, 2011.

X. Chen, K. Gatsis, H. Hassani and S. S. Bidokhti, “Age of information in random access channels” *arXiv preprint arxiv: 1912.01473,* 2019.

7. APPENDİX : The Proof of Lemma 2

We will begin the proof for the *s* values $s = 1, 2, \dots, \Gamma - 1$. The properties *(i)* and *(ii)* directly follow from Proposition 4 *(i)*, where $\pi(S_1^P) = \pi_{m_1}$ and $\pi(S_2^P) = \pi_{m_2}$. Although Property *(iii)* follows from the same property, it is not directly seen:

$$\begin{aligned}\lim_{n\to\infty} \frac{\pi(S_1^{\mathbf{P}})}{n\,\pi(S_2^{\mathbf{P}})} &= \lim_{n\to\infty} \frac{\pi_{m_1}}{n\pi_{m_1-1}} \\ &\overset{(a)}{=} \lim_{n\to\infty} \frac{(1-(m_1-1)\tau(1-\tau)^{m_1-2} - (m_1-1)\tau\tau_2[(1-\tau\tau_2)^{m_1-2} - (1-\tau)^{m_1-2}])}{n\tau(1-\tau)^{m_1-1} + n\tau\tau_2[(1-\tau\tau_2)^{m_1-1} - (1-\tau)^{m_1-1}]}. \\ &= \frac{1}{\alpha e^{-k\alpha} + \alpha\tau_2(e^{-\tau_2 k\alpha} - e^{-k\alpha})} - k\end{aligned}$$

where the step (a) follows from the π_m/π_{m-1} expression in part 4.3.3.

Next, we move on to the *s* value $s = \Gamma$ and show that the properties still hold. We will start with showing that $\pi(S_1^P) = \pi_{m_1}$. Assuming that $1 \notin \{u_1, u_2, \dots, u_{n-m_1-1}\}$holds and S_1^P is the current state, the previous state can be one of the following types:

- $(\Gamma - 1, m_1, \{u_1 - 1, u_2 - 1, \dots, u_{n-m_1} - 1\})$
- $(\Gamma - 1, m_1 - 1, \{\Gamma - 1, u_1 - 1, u_2 - 1, \dots, u_{n-m_1} - 1\})$

In Proposition 4 *(ii)*, the steady state probabilities of these types are given as π_{m_1} and π_{m_1-1}, respectively. The steady state probability of S_1^P can be calculated using the given probabilities for the preceding state and their transition probabilities as:

$$\begin{aligned}\pi(S_1^{\mathbf{P}}) &= \pi_{m_1}(1 - m_1\tau(1-\tau)^{m_1-1} - m_1\tau\tau_2[(1-\tau\tau_2)^{m_1-1} - (1-\tau)^{m_1-1}]) \\ &+\pi_{m_1-1}m_1(1-(m_1-1)\tau(1-\tau)^{m_1-2} - (m_1-1)\tau\tau_2[(1-\tau\tau_2)^{m_1-2} - (1-\tau)^{m_1-2}]) \\ &= \pi_{m_1}\end{aligned}$$

where the π_{m_1} result is obtained through the ratio given in the π_m/π_{m-1} expression in part 4.3.3. Now that we are done with the case of $1 \notin \{u_1, u_2, \ldots, u_{n-m_1-1}\}$, we move on to the case $1 \in \{u_1, u_2, \ldots, u_{n-m_1-1}\}$. We will assume $u_{n-m_1-1} = 1$ without loss of generality and then follow similar steps with the preceding case. The previous state can be one of the following this time:

- $(\Gamma - 1, m_1 + 1, \{u_1 - 1, u_2 - 1, \ldots, u_{n-m_1-2} - 1\})$
- $(\Gamma - 1, m_1, \{\Gamma - 1, u_1 - 1, u_2 - 1, \ldots, u_{n-m_1-2} - 1\})$

Again, using Proposition 4 *(ii)*, we find the steady state probabilities of these states as π_{m_1+1} and π_{m_1}, respectively. Then, the steady state probability of S_1^P is derived using the transition probabilities as:

$$\begin{aligned}\pi(S_1^{\mathbf{P}}) &= \pi_{m_1+1}(\tau(1-\tau)^{m_1} + \tau\tau_2[(1-\tau\tau_2)^{m_1} - (1-\tau)^{m_1}]) \\ &+\pi_{m_1}(m_1\tau(1-\tau)^{m_1-1} - m_1\tau\tau_2[(1-\tau\tau_2)^{m_1-1} - (1-\tau)^{m_1-1}]) \\ &= \pi_{m_1}\end{aligned}$$

$\pi(S_1^P) = \pi_{m_2}$ since there is a symmetry. The properties *(i)* and *(ii)* follow from Proposition 4 *(i)* and Property *(iii)* follows from the $\lim_{n\to\infty} \frac{\pi(S_1^P)}{n\pi(S_2^P)}$ expression at the beginning of this part.

The last case of ranges for the *s* value is$\forall s \geq \Gamma$. In order to show that the lemma still holds for this case, we will use induction. The preceding case $s = \Gamma$ is the initial case and is already covered. Therefore, we assume that $s > \Gamma$ and that the properties of the lemma holds for all the smaller values of *s*. Here we will again use two cases two make our analysis:

Case 1. If $1 \notin \{u_1, u_2, \ldots, u_{n-m_1-1}\}$

For the sake of readability, the probability expressions are shortened in the following way:

$$\begin{aligned}\pi_m^{(s)} &= \pi(s, m, \{u_1, u_2, \ldots, u_{n-m-1}\}) = \pi(S_1^{\mathbf{P}}) \\ \pi_m^{(s-1)} &= \pi(s-1, m, \{u_1 - 1, u_2 - 1, \ldots, u_{n-m-1} - 1\}) = \pi(Q_1^{\mathbf{P}}) \\ \pi_{m-1}^{(s-1)} &= \pi(s-1, m-1, \{\Gamma - 1, u_1 - 1, u_2 - 1, \ldots, u_{n-m-1} - 1\})\end{aligned}$$

A state of type $(s, m, \{u_1, u_2, \ldots, u_{n-m_1-1}\})$ can be preceded by states with probabilities $\pi_m^{(s-1)}$ or $\pi_{m-1}^{(s-1)}$. Then, the value of $\pi_m^{(s)}$ can be calculated using the transition probabilities as:

$$\pi_m^{(s)} = \pi_m^{(s-1)}(1-(m+1)\tau(1-\tau)^m-(m+1)\tau\tau_2[(1-\tau\tau_2)^m-(1-\tau)^m]) + \pi_{m-1}^{(s-1)}(m+1)(1-m\tau(1-\tau)^{m-1}-m\tau\tau_2[(1-\tau\tau_2)^{m-1}-(1-\tau)^{m-1}])$$

Then,

$$\begin{aligned}
\lim_{n\to\infty}\frac{\pi_m^{(s)}}{\pi_m^{(s-1)}} &= \lim_{n\to\infty}\frac{\pi_m^{(s-1)}(1-(m+1)\tau(1-\tau)^m-(m+1)\tau\tau_2[(1-\tau\tau_2)^m-(1-\tau)^m])}{\pi_m^{(s-1)}} \\
&\quad + \frac{\pi_{m-1}^{(s-1)}(m+1)(1-m\tau(1-\tau)^{m-1}-m\tau\tau_2[(1-\tau\tau_2)^{m-1}-(1-\tau)^{m-1}])}{\pi_m^{(s-1)}} \\
&= \lim_{n\to\infty} 1-(m+1)\tau(1-\tau)^m-(m+1)\tau\tau_2[(1-\tau\tau_2)^m-(1-\tau)^m] \\
&\quad + \frac{\pi_{m-1}^{(s-1)}}{\pi_m^{(s-1)}}(m+1)(1-m\tau(1-\tau)^{m-1}-m\tau\tau_2[(1-\tau\tau_2)^{m-1}-(1-\tau)^{m-1}]) \\
&= \lim_{n\to\infty} 1-\frac{m+1}{n}(n\tau)(1-\tau)^m-\frac{m+1}{n}(n\tau)\tau_2[(1-\tau\tau_2)^m-(1-\tau)^m] \\
&\quad + \frac{n\,\pi_{m-1}^{(s-1)}}{\pi_m^{(s-1)}}\frac{m+1}{n}(1-\frac{m}{n}(n\tau)(1-\tau)^{m-1}-\frac{m}{n}(n\tau)\tau_2[(1-\tau\tau_2)^{m-1}-(1-\tau)^{m-1}]) \\
&\overset{(a)}{=} \lim_{n\to\infty} 1-k\alpha e^{-k\alpha}-k\alpha\tau_2[e^{-\tau_2 k\alpha}-e^{-k\alpha}] \\
&\quad + \frac{1}{\frac{1}{\alpha e^{-k\alpha}+\alpha\tau_2(e^{-\tau_2 k\alpha}-e^{-k\alpha})}-k}k(1-k\alpha e^{-k\alpha}-k\alpha\tau_2[e^{-\tau_2 k\alpha}-e^{-k\alpha}]) = 1
\end{aligned}$$

where *(a)* follows from property *(iii)*.

Case 2. If $1 \in \{u_1, u_2, \ldots, u_{n-m_1-1}\}$ and without loss of generality we choose $u_{n-m-1} = 1$.

Again, for the sake of readability, the probability expressions are shortened in the following way:

$$\begin{aligned}
\pi_m^{(s)} &= \pi(s, m, \{u_1, u_2, \ldots, u_{n-m-2}, 1\}) = \pi(S_1^{\mathbf{P}}) \\
\pi_m^{(s-1)} &= \pi(s-1, m, \{\Gamma-1, u_1-1, u_2-1, \ldots, u_{n-m-2}-1\}) = \pi(Q_1^{\mathbf{P}}) \\
\pi_{m+1}^{(s-1)} &= \pi(s-1, m+1, \{u_1-1, u_2-1, \ldots, u_{n-m-2}-1\})
\end{aligned}$$

A state of type $(s, m, \{u_1, u_2, \ldots, u_{n-m_1-2}, 1\})$ can be preceded by two types of states with steady state probabilities $\pi_m^{(s-1)}$ and $\pi_{m+1}^{(s-1)}$. Then, using the transition probabilities, the value of $\pi_m^{(s)}$ is obtained as:

$$\pi_m^{(s)} = \pi_{m+1}^{(s-1)}(\tau(1-\tau)^m+\tau\tau_2[(1-\tau\tau_2)^m-(1-\tau)^m]) + \pi_m^{(s-1)}(m\tau(1-\tau)^{m-1}-m\tau\tau_2[(1-\tau\tau_2)^{m-1}-(1-\tau)^{m-1}])$$

Then,

$$\begin{aligned}
\lim_{n\to\infty}\frac{\pi_m^{(s)}}{\pi_m^{(s-1)}} &= \lim_{n\to\infty}\frac{\pi_{m+1}^{(s-1)}(\tau(1-\tau)^m+\tau\tau_2[(1-\tau\tau_2)^m-(1-\tau)^m])}{\pi_m^{(s-1)}} \\
&\quad+\frac{\pi_m^{(s-1)}(m\tau(1-\tau)^{m-1}-m\tau\tau_2[(1-\tau\tau_2)^{m-1}-(1-\tau)^{m-1}])}{\pi_m^{(s-1)}} \\
&= \lim_{n\to\infty}\frac{\pi_{m+1}^{(s-1)}}{\pi_m^{(s-1)}}(\tau(1-\tau)^m+\tau\tau_2[(1-\tau\tau_2)^m-(1-\tau)^m]) \\
&\quad+(m\tau(1-\tau)^{m-1}-m\tau\tau_2[(1-\tau\tau_2)^{m-1}-(1-\tau)^{m-1}]) \\
&= \lim_{n\to\infty}\frac{\pi_{m+1}^{(s-1)}}{n\pi_m^{(s-1)}}((n\tau)(1-\tau)^m+(n\tau)\tau_2[(1-\tau\tau_2)^m-(1-\tau)^m]) \\
&\quad+(\frac{m}{n}(n\tau)(1-\tau)^{m-1}-\frac{m}{n}(n\tau)\tau_2[(1-\tau\tau_2)^{m-1}-(1-\tau)^{m-1}]) \\
&= \lim_{n\to\infty}(\frac{1}{\alpha e^{-k\alpha}+\alpha\tau_2(e^{-\tau_2 k\alpha}-e^{-k\alpha})}-k)(\alpha e^{-k\alpha}+\alpha\tau_2[e^{-\tau_2 k\alpha}-e^{-k\alpha}]) \\
&\quad+(k\alpha e^{-k\alpha}-k\alpha\tau_2[e^{-\tau_2 k\alpha}-e^{-k\alpha}])=1
\end{aligned}$$

With the last case, we completed the proof of property *(i)*. Now, for the case $m_1=m_2$,

$$\begin{aligned}
\lim_{n\to\infty}\frac{\pi(S_1^{\mathbf{P}})}{\pi(S_2^{\mathbf{P}})} &= \lim_{n\to\infty}\frac{\pi(S_1^{\mathbf{P}})}{\pi(Q_1^{\mathbf{P}})}\frac{\pi(Q_2^{\mathbf{P}})}{\pi(S_2^{\mathbf{P}})}\frac{\pi(Q_1^{\mathbf{P}})}{\pi(Q_2^{\mathbf{P}})} \\
&\overset{(a)}{=} \lim_{n\to\infty}\frac{\pi(Q_1^{\mathbf{P}})}{\pi(Q_2^{\mathbf{P}})} \overset{(b)}{=} 1
\end{aligned}$$

Since the state of the pivot source for both the states Q_1^P and Q_2^P is *s-1* and number of active sources is m_1 and m_2 respectively, *(a)* follows from property *(i)* and *(b)* follows from property *(ii)*.

Similarly, for the case $m_1=m_2+1$,

$$\begin{aligned}
\lim_{n\to\infty}\frac{\pi(S_1^{\mathbf{P}})}{\pi(n\,S_2^{\mathbf{P}})} &= \lim_{n\to\infty}\frac{\pi(S_1^{\mathbf{P}})}{\pi(Q_1^{\mathbf{P}})}\frac{\pi(Q_2^{\mathbf{P}})}{\pi(S_2^{\mathbf{P}})}\frac{\pi(Q_1^{\mathbf{P}})}{n\,\pi(Q_2^{\mathbf{P}})} \\
&\overset{(a)}{=} \lim_{n\to\infty}\frac{\pi(Q_1^{\mathbf{P}})}{n\,\pi(Q_2^{\mathbf{P}})} \\
&\overset{(b)}{=} \frac{1}{\alpha e^{-k\alpha}+\alpha\tau_2(e^{-\tau_2 k\alpha}-e^{-k\alpha})}-k
\end{aligned}$$

Since the state of the pivot source for both the states Q_1^P and Q_2^P is *s-1* and number of active sources is m_1 and m_2 respectively, *(a)* follows from property *(i)* and *(b)* follows from property *(iii)*.